PHYSICAL REVIEW D **87,** 115012 (2013)

LHC-7 supersymmetry search interpretation within the phenomenological MSSM

Shehu S. AbdusSalam*

The Abdus Salam International Centre for Theoretical Physics, Strada Costiera 11, Trieste 34014, Italy

(Received 19 March 2013; published 10 June 2013)

The ATLAS Collaboration published supersymmetry limits based on up to about 4.7 fb^{-1} data collected over the year 2011 from LHC runs at 7 TeV. These were mainly interpreted within restricted, particular or simplified models for supersymmetry breaking schemes or scenarios. The phenomenological MSSM (pMSSM) is an alternative and more generic supersymmetry framework that captures broader phenomenological features. Searching for more generic conclusions from the supersymmetry limits interpretation, we update a Bayesian global fit of the pMSSM to pre-LHC data using the LHC-7 limits. The posterior distributions show the most up-to-date features, revealing allowed versus excluded regions in sparticle mass planes within the MSSM.

DOI: 10.1103/PhysRevD.87.115012 PACS numbers: 12.60.Jv

I. INTRODUCTION

The discovery of the Higgs boson–like state around 126.5 [1] or 125 GeV [2] at the Large Hadron Collider (LHC) is an excellent accomplishment. However, this only marks the beginning of exciting moments for particle physics's endeavor to establish the mechanism of electroweak symmetry breaking and to shed light on new physics beyond the standard model (BSM) During the year 2011 run of the LHC machine, both ATLAS and CMS detectors have recorded up to about 5 fb^{-1} of data. The collaborations have conducted many analyses on the data, searching for, amongst other new physics models, supersymmetry (SUSY) by looking for final states containing jets and large missing transverse energy (MET) that could indicate the production of squarks and gluinos in the collider. According to public results, there is no sign of SUSY being observed as of the time of writing this article. As such findings of the experiments were presented in the form of model-independent non-SM cross section limits and interpreted by showing exclusion regions within specific models of SUSY, such as the constrained version of the R-parity conserving minimal supersymmetric standard model (MSSM) called CMSSM/mSUGRA, particular SUSY breaking schemes (for a review see e.g. [3]) or simplified models [4] of SUSY scenarios.

A. Aim of this paper

In this paper we will assess the impact of the LHC-7 SUSY results on the R-parity conserving phenomenological MSSM (pMSSM). In particular, we are going to use the ATLAS SUSY limits reported in Refs. [5–15] to discriminate between allowed and excluded regions in the pMSSM sparticle mass planes. To date several research groups have looked into analyzing the impact of LHC-7 data on various SUSY models. For nonexhaustive instances, see Refs. [16–34]. Out of these, the interpretation, within the pMSSM for the CMS Collaboration's SUSY limits based on 1 fb^{-1} data presented in [21] has a particular relevance. Our analyses update the impact of LHC results on the pMSSM, hereby using SUSY limits from the ATLAS Collaboration with up to about 4.7 fb^{-1} data. Following the approach in Ref. [21], the data d from the various experiments used for our analyses are decomposed into two independent parts,

$$d = d_{\text{pre-LHC}} \oplus d_{\text{LHC}}, \tag{1}$$

where $d_{\text{pre-LHC}}$ represents the indirect pre-LHC collider and cold dark matter relic density constraints summarized in Table I and d_{LHC}, the LHC-7 SUSY limits shown in Table II. The pMSSM posterior distributions from the Bayesian global fit [47] to pre-LHC data are now used as the prior, $\pi(\theta)$, for updating the pMSSM posterior sample with the LHC SUSY limits. Using Bayes theorem, weighing the prior with the likelihood over the LHC data $L(d_{\text{LHC}}|\theta)$, gives an updated, post-LHC, posterior distribution,

$$p(\theta|d_{\text{LHC}}) \sim L(d_{\text{LHC}}|\theta)\pi(\theta), \tag{2}$$

valid up to a normalization factor. Analyzing this will reveal information about the impact of the LHC-7 data on the pMSSM parameter space.

This paper is structured as follows. In the remaining part of this section we give a brief recapitulation of the Bayesian global fit of the pMSSM to the pre-LHC data, allowing us to set the context for explaining our analyses. In Sec. II we present the methodology employed in simulating the SUSY event at the LHC and the computation of the pMSSM predictions for the cross section within acceptance, the main observable to compare with the upper limits from ATLAS. The impact of the experimental limits on the pMSSM is presented in Sec. III. The last section is reserved for discussing our conclusions and outlook.

*shehu@ictp.it

TABLE I. Summary for the central values and errors for the electroweak physics observables, B-physics observables and cold dark matter relic density constraints. The posterior distribution from the pre-LHC fit for $\mathrm{Br}(B_s \to \mu^+\mu^-)$ is centered around 2.8×10^{-9} so most of the points are in agreement with the more recent bound 4.5×10^{-9} [35].

Observable	Constraint
m_W [GeV]	80.399 ± 0.027 [36]
Γ_Z [GeV]	2.4952 ± 0.0025 [37]
$\sin^2\theta^{\mathrm{lep}}_{\mathrm{eff}}$	0.2324 ± 0.0012 [37]
δa_μ	$(30.2 \pm 9.0) \times 10^{10}$ [38,39]
R^0_l	20.767 ± 0.025 [37]
R^0_b	0.21629 ± 0.00066 [37]
R^0_c	0.1721 ± 0.0030 [37]
A^b_{FB}	0.0992 ± 0.0016 [37]
A^c_{FB}	0.0707 ± 0.035 [37]
$A^l = A^e$	0.1513 ± 0.0021 [37]
A^b	0.923 ± 0.020 [37]
A^c	0.670 ± 0.027 [37]
$\mathrm{Br}(B \to X_s\gamma)$	$(3.55 \pm 0.42) \times 10^4$ [40]
$\mathrm{Br}(B_s \to \mu^+\mu^-)$	$<5.8 \times 10^{-8}$ (see caption.)
$R_{\Delta M_{B_s}}$	0.85 ± 0.11 [41]
$R_{\mathrm{Br}(B_u \to \tau\nu)}$	1.26 ± 0.41 [42–44]
Δ_{0-}	0.0375 ± 0.0289 [45]
$\Omega_{\mathrm{CDM}}h^2$	0.11 ± 0.02 [46]

B. The pre-LHC pMSSM fit review

The Bayesian global fit of the pMSSM to pre-LHC data was performed in [47,48]. The posterior samples reveal SUSY spectra with various characteristics, satisfying different phenomenological scenarios [49–51] that are mainly difficult to capture within the classic constrained benchmark models. For the pMSSM fit, the parametrization is completely decoupled from the details of the physics responsible for SUSY breaking. Requiring compatibility with observations about CP violation and flavor changing neutral current processes, only real soft SUSY breaking terms are considered, with all off-diagonal elements in the sfermion mass terms and trilinear couplings set to zero, and the first-and second-generation soft terms equalized, leading to a set of 20 parameters,

$$\theta = \left\{ M_{1,2,3}; m^{\text{3rd gen}}_{\tilde{f}_{Q,U,D,L,E}}, m^{\text{1st/2nd gen}}_{\tilde{f}_{Q,U,D,L,E}}; A_{t,b,\tau,\mu=e}, m^2_{H_{u,d}}, \tan\beta \right\}, \tag{3}$$

where M_1, M_2 and M_3 are the gaugino mass parameters (allowed in the range -4 to 4 TeV) and $m_{\tilde{f}}$ are the sfermion mass parameters (allowed in the range 100 GeV to 4 TeV). $A_{t,b,\tau,\mu=e} \in [-8, 8]$ TeV represent the trilinear scalar couplings, while the Higgs-sector parameters are specified by the two Higgs doublet masses $m^2_{H_1}$, $m^2_{H_2}$ (with $m^2 \in \mathrm{sign}(m)[-4, 4]^2$ TeV^2), the ratio of the vacuum expectation values $\tan\beta = \langle H_2\rangle/\langle H_1\rangle$ (allowed between 2 and 60) and the sign of the Higgs doublets mixing parameter, $\mathrm{sign}(\mu)$ (randomly ± 1.) The pre-LHC data, $d_{\text{pre-LHC}} = \underline{\delta} = \{\mu_i, \sigma_i\}$, where $i = 1, 2, \ldots$, represents the experimental central values and errors (summarized in Table I) for the electroweak physics observables, B-physics observables and the cold dark matter relic density observable. These together form the observables set,

$$\begin{aligned} \underline{O} = \{ & m_W, \sin^2\theta^{\mathrm{lep}}_{\mathrm{eff}}, \Gamma_Z, \delta a_\mu, R^0_l, A^{0,l}_{fb}, A^l = A^e, R^0_{b,c}, A^{b,c}_{fb}, \\ & A^{b,c}, \mathrm{BR}(B \to X_s\gamma), \mathrm{BR}(B_s \to \mu^+\mu^-), \Delta_{0-}, \\ & R_{\mathrm{BR}(B_u \to \tau\nu)}, R_{\Delta M_{B_s}}, \Omega_{\mathrm{CDM}}h^2 \}. \end{aligned} \tag{4}$$

The pre-LHC posterior distribution from the Bayesian global fit which is now considered as a prior distribution for the update with the LHC data is given by

TABLE II. The ATLAS 95% C.L. upper limits on the extra-SM cross sections within acceptance for the various signal regions described in the text. The limits on each search channel row are ordered, with the first representing the first corresponding name of the signal region described in the corresponding experimental paper. The unit for each cross section is the inverse of the corresponding luminosity.

Channels + MET	Signal regions, σ_{BSM} upper limits											Luminosity
jets + 0-lep	1.3	0.35	1.1	0.11	⋯	⋯	⋯	⋯	⋯	⋯	⋯	35 pb^{-1} [5]
jets + 0-lep	22	25	429	27	17	⋯	⋯	⋯	⋯	⋯	⋯	1.04 fb^{-1} [9]
$\geq$6 jets	194	8.4	12.2	4.5	⋯	⋯	⋯	⋯	⋯	⋯	⋯	1.34 fb^{-1} [10]
0 jet + 2-lep	0.22	0.09	0.21	0.07	0.07	0.07	⋯	⋯	⋯	⋯	⋯	35 pb^{-1} [6]
jets + 1-lep	41	53	⋯	⋯	⋯	⋯	⋯	⋯	⋯	⋯	⋯	165 pb^{-1} [7]
b-jet + 0-lep	288	61	78	17	⋯	⋯	⋯	⋯	⋯	⋯	⋯	830 pb^{-1} [8]
$\geq$(2–6)jets + 0-lep	0.62	5.3	6.2	0.65	3.5	3.7	12	2.2	2.6	2.5	18	4.7 fb^{-1} [11]
$\geq$(6–9)jets + 0-lep	14	4.2	1.2	9.8	3.2	0.81	⋯	⋯	⋯	⋯	⋯	4.7 fb^{-1} [12]
$\geq$(2–4)jets + 1-lep	1.3	1.5	3.7	⋯	⋯	⋯	⋯	⋯	⋯	⋯	⋯	4.7 fb^{-1} [13]
$\geq$(1–2)b-jets + 0-lep	283	65	15.4	61	14.4	4.3	22.2	8.5	⋯	⋯	⋯	2.05 fb^{-1} [14]
3-lep	3.5	1.5	⋯	⋯	⋯	⋯	⋯	⋯	⋯	⋯	⋯	2.06 fb^{-1} [15]

$$\pi(\theta) = \pi'(\theta)\prod_{i=1}(2\pi\sigma_i^2)^{-1/2}\exp[-(O_i - \mu_i)^2/2\sigma_i^2], \quad (5)$$

where $\pi'(\theta)$ is the prior probability density for the Bayesian global fits to $d_{\text{pre-LHC}}$, which can be flat over the individual parameters θ_i (for flat prior fits) or flat over the logarithm of the parameters, $\log\theta$ (for log prior fits). Here we do not aim at checking the constraining strength of the LHC data over the pMSSM parameters. Thus, no prior dependence analysis is discussed and we work with only the log prior posterior samples of the pre-LHC global fits. In the next section, we describe the data, i.e. the extra-SM cross sections within acceptance, the simulation of SUSY events at the LHC and the ATLAS-like analysis of the events. These are used in constructing the likelihood, $L(d_{\text{LHC}}|\theta)$, required in addition to the prior, $\pi(\theta)$, for completing the required variables in the target Eq. (2).

II. ANALYSIS

Our analysis is centered around computing the likelihood for d_{LHC}, given the pMSSM parameters, θ_i. In this section we describe the ATLAS data and the simulation of SUSY events. The latter allows for computing the extra-SM, here SUSY, cross sections within acceptances, σ^{acc}, over various cuts on the collider final state characteristics. The degree of agreement or deviation between the pMSSM predictions for σ^{acc} and the experimental values is used to quantify the plausibility of obtaining the data from the model parameters, $L(d_{\text{LHC}}|\theta)$.

A. The data, d_{LHC}

The LHC data we use are the 95% C.L. upper limits on the non-SM cross section within acceptance. For each of the ATLAS analyses [5–15], there are various signal regions defined by a specific set of cuts and events selection criteria. The results are based on various, namely 35 pb^{-1} up to 4.7 fb^{-1}, data sets recorded by the ATLAS detector at 7 TeV center-of-mass energy run of the LHC in the year 2011. The analyses were designed to capture different possible manifestations of SUSY after the proton-proton collisions at the LHC.

SUSY production at the collider would be dominated by large direct production of squark and gluino pairs ($\tilde{g}\,\tilde{g}$, $\tilde{g}\,\tilde{q}$, or $\tilde{q}\,\tilde{q}$) that would decay ($\tilde{q} \to q\tilde{\chi}_1^0$ and $\tilde{g} \to q\tilde{q}\tilde{\chi}_1^0$) to the weakly interacting neutralino lightest supersymmetric particle (LSP), $\tilde{\chi}_1^0$, which escapes the detector unseen in the form of missing transverse energy, MET. The different groups of search channels, which we briefly describe here, are all MET-based. The first is the search for squarks and gluinos that lead to final states containing high-p_T jets, MET and no leptons (electrons or muons), as in Refs. [5,9–12]. The strategy for this group of searches is optimized for maximal discovery reach in the $m_{\tilde{g}}$-$m_{\tilde{q}}$ plane. This group of search channels could be specialized to the case of having heavy flavor jets. Doing this would capture the scenario where the sbottoms ($\tilde{b}_1$) and stops ($\tilde{t}_1$) are lighter than other squarks so that direct or gluino-mediated production ($\tilde{g} \to b\tilde{b}$ or $\tilde{g} \to t\tilde{t}$) is the dominant SUSY production mode in the collider as considered in Refs. [8,14].

Requiring final states containing one (or more) electrons or muons in addition to jets and MET would capture scenarios where gluinos cascade decay products include a charginos, $\tilde{\chi}^{\pm}$, which subsequently decays into final states containing high-p_T leptons, as considered in Refs. [7,13]. Further, in a scenario such as natural SUSY [52], where first- and second-generation sfermion masses are larger than a few TeVs, the direct production of weak gauginos may be the dominant SUSY processes. When both gauginos decay leptonically, a distinctive signature with no jets, three leptons and significant MET, as considered in Ref. [15], can be observed.

In all, we considered 55 SUSY signal regions. For each region, the number of events that pass the selected criteria and also the expected standard model (background) events were reported. In addition, the upper bounds on the cross sections for non-SM interactions were also given. These allow for comparisons with any BSM predictions to determine whether the new physics model is allowed or ruled out (based on the particle-level cuts without detector simulation) at the 95% confidence level. This is the approach we have chosen. The LHC data, d_{LHC}, for our analysis is represented by the set summarized in Table II. The limits are used to constrain the pMSSM σ^{acc} predictions from the simulation of SUSY production at the LHC.[1]

B. The pMSSM predictions for the cross section within acceptance, σ_i^{acc}

In order to compute the predictions for σ_i^{acc} within acceptances over the cuts and selections criteria that define the various ATLAS SUSY signal regions, we simulate the generation of SUSY events at 7 TeV LHC using the Monte Carlo events generator and then analyze the collider final states in a similar fashion to the ATLAS procedures.

1. SUSY events simulation

We use HERWIG++ [58,59] to simulate four sets of sparticle production processes for each point in the pMSSM

[1]References [53,54] extend [14,15] with 4.7 fb^{-1} data, but the publications were made at a time when our simulations cannot be aborted for making and including new analysis codes. No change in our conclusions is expected from these updates of relatively less constraining search channels. Therefore, the updates are not considered here as they are not worthy of the repetition of expensive simulations done before their publication. Similarly, including in our analysis the extensions of results [11–13] to those in [55–57] with 5.8 fb^{-1} data will require repetition of simulations with change of collision energy to 8 TeV, whereas the focus here is on the 7 TeV results.

sample, namely, (a) squark-squark and squark-gluino production, (b) the production of an electroweak gaugino in association with a squark or gluino, and (c) the production of slepton and electroweak gaugino pairs. Each of the pMSSM posterior sample points in the SUSY Les Houches accord (SLHA) file format produced by SOFTSUSY [60] is passed to HERWIG++ [58,59] for generating 1000 SUSY events. Throughout the analysis we use the SUSY production cross section from the event generator, calculated at leading order in perturbative QCD.[2]

2. Analyzing the simulated SUSY events using RIVET

The analysis of the generated SUSY events is done at the particle level using the "Robust Independent Validation of Experiment and Theory" (RIVET) Monte Carlo validation framework [61]. We use this to z each and every SUSY event generated by the Monte Carlo collider simulator, without the need for detector simulations and the publicly available RIVET analyses for the ATLAS SUSY searches in Refs. [5–15]. The Rivet analyses are plugged in to HERWIG++ for computing the acceptances, $A_i = N_{\rm cuts}/N_{\rm total}$, after applying the various cuts on the kinematic variables of the collider final states. Here $N_{\rm cuts}$ is the number of events that pass the experimental cuts and $N_{\rm total} = 1000$ is the total number of generated SUSY events. RIVET acts per event on the events produced by HERWIG++. The jet identification is done using FASTJET [62]. The cross section within acceptance is computed as

$$\sigma_i^{\rm acc} = \epsilon A_i \sigma_i^{\rm SUSY,LO}, \tag{6}$$

where we consider the efficiency, $\epsilon = 1$ (since no detector simulation); $i = 1, 2, \ldots, 55$ runs over the 55 different signal regions, and $\sigma^{\rm SUSY,LO}$ is the total LO SUSY production cross section.

C. The likelihood, $L(d_{\rm LHC}|\theta)$

The likelihood is a simple step function that equals unity if the ATLAS limits are satisfied; otherwise, it equals zero if excluded. SUSY points with predicted cross sections smaller (greater) than the ATLAS non-SM limits are then allowed (excluded) at 95% confidence level according to

$$L(d_{\rm LHC}|\theta) = \prod_{i=1}^{55} \ell_i; \qquad \ell_i = \left\{ \begin{array}{ll} 0 & \text{if } \sigma_i^{\rm acc} > \sigma_i^{\rm acc,max} \\ 1 & \text{if } \sigma_i^{\rm acc} \leq \sigma_i^{\rm acc,max} \end{array} \right\}. \tag{7}$$

[2]About half of the posterior samples we consider have a negative gluino mass, allowed by the SLHA accord, that crashes the PROSPINO NLO calculator. As such the NLO correction is dropped out.

TABLE III. Summary of the relative number of surviving posterior points, from the pre-LHC Bayesian global fits of the pMSSM, and after imposing the Higgs discovery data and SUSY limits.

No.	Constraint	Log prior survive
1.	$m_h = 122$–128 GeV	36.08%
2.	$m_h = 125$–126.5 GeV	9.17%
3.	SUSY $\sigma^{\rm acc}$ limits	57.47%
4.	$m_h(1)$ and SUSY $\sigma^{\rm acc}$ limits	14.53%
5.	1.67-σ $R_{ZZ;\gamma\gamma}$	13.30%
6.	$m_h(1)$ & 1.67-σ $R_{ZZ;\gamma\gamma}$	4.67%
7.	1.67-σ $R_{ZZ;\gamma\gamma}$ & SUSY $\sigma^{\rm acc}$ limits	6.11%
8.	m_h, 1.67-σ $R_{ZZ;\gamma\gamma}$ & SUSY $\sigma^{\rm acc}$ limits	2.19%

III. THE SUSY LIMITS' IMPACT ON THE PMSSM

The relative number of the pMSSM points that survive the SUSY limits, in various combinations with the Higgs-sector data (in the di-photon channels as applied in Ref. [63] and other ATLAS, CMS, LEP and Tevatron Higgs-sector constraints implemented in the HEP packages HIGGSBOUNDS [64] and FEYNHIGGS [65]), are summarized in Table III. The posterior probability distribution for the sparticle masses derived from the post-LHC distribution Eq. (2) are shown in Fig. 1. As can be seen from the mentioned plots, the ATLAS SUSY limits are most sensitive in constraining the gluino mass whose central value is now shifted[3] from around 2 to 3 TeV followed by the squark masses. The effect of the SUSY limits on the gluino mass seems to be very different from what happens for the case of constrained models such as CMSSM/mSUGRA (addressing this is outside the scope of this paper). The limits are relatively less sensitive in constraining sleptons, electroweak gauginos and the lighter sbottom or stop quarks. The resultant effect of applying the limits coming from the 55 different ATLAS SUSY signal regions shown in Table II on the pMSSM can be summarized in plots showing allowed versus ruled out regions in sparticle mass planes such as the ones shown in Fig. 2. The spectra used in generating Fig. 2 are compatible with all other experimental constraints shown in Table I. The plots give a non-Bayesian view of the effect of the SUSY limits on the presented mass planes. Points with $\frac{\sigma_i^{\rm acc}}{\sigma_i^{\rm acc,max}} > 1$ are excluded at 95% C.L. The color shading reveals the following spectrum of exclusion strength: from being strongly ruled out [color-coded black, for regions with $\frac{\sigma_i^{\rm acc}}{\sigma_i^{\rm acc,max}} \geq \mathcal{O}(10)$] to mildly allowed within uncertainties [color-coded white, yellow or brown, for regions with $\frac{\sigma_i^{\rm acc}}{\sigma_i^{\rm acc,max}} \lesssim \mathcal{O}(1-2)$]. The excluded regions have very high sparticle production

[3]The SUSY search channels that involve final states with high number of jet multiplicities severely constrains the gluino mass to higher values relative to the pre-LHC mass distribution.

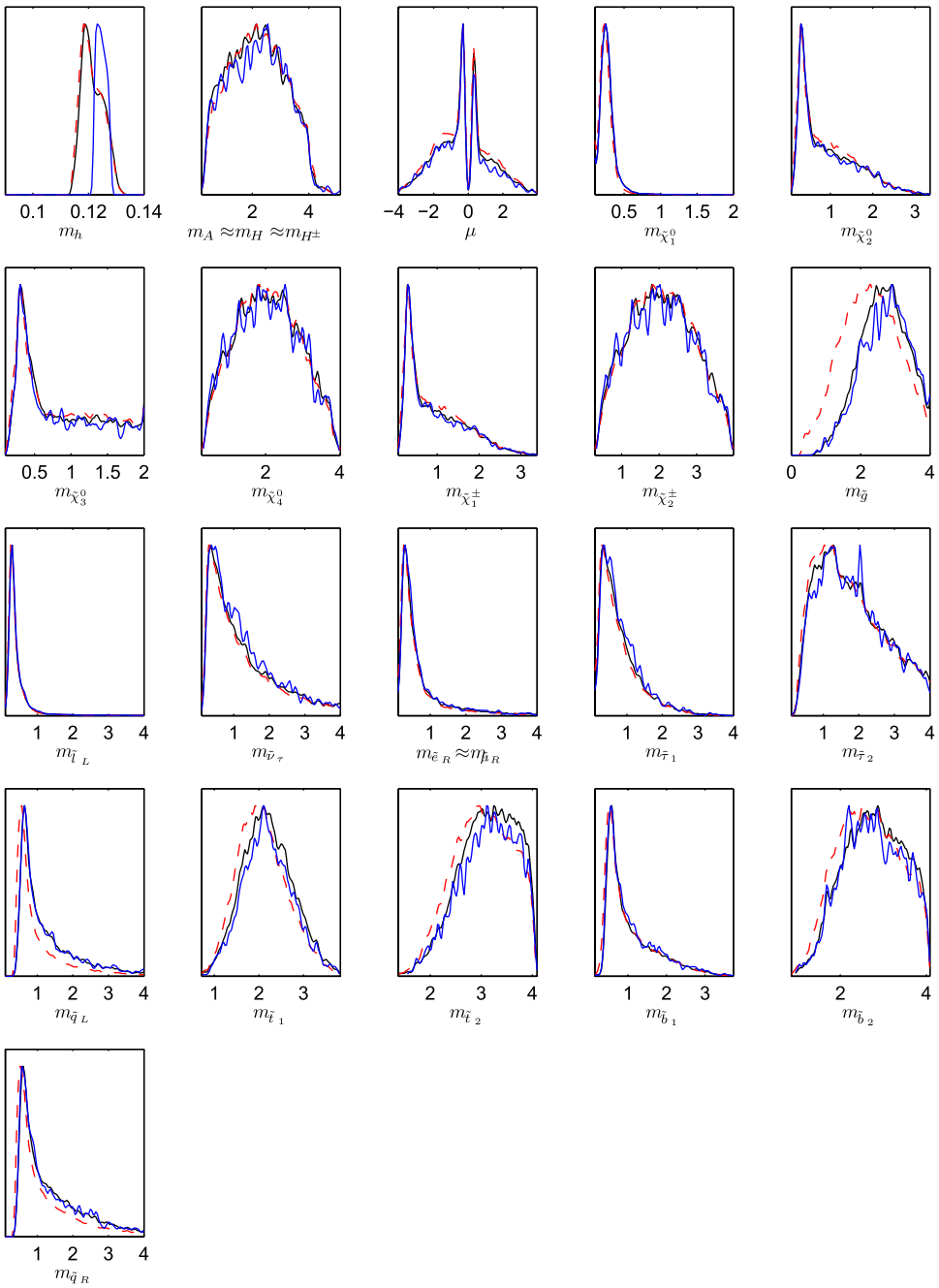

FIG. 1 (color online). The plots compare the log prior pMSSM sparticle masses' marginalized one-dimensional pre-LHC posterior distributions (dashed red curves) and the surviving parameter regions after imposing only the SUSY limit (black curves) and both $m_h = 122.0$–128.0 GeV and SUSY limits together (blue curves). All the masses are in TeV units. The vertical axes represent the relative probability weights of the model points.

cross sections compared to the experimental limits in Table II. It should be noted that the plots are expected to be irregular for being two-dimensional slices over a non-smooth 32-dimensional space of sparticle masses. In addition, it apparently looks logical that some of the high-mass regions in the presented planes should not have been ruled out. But such regions can, indeed, be ruled out if the corresponding sparticle spectrum has high total SUSY production cross section due to perhaps a light state(s) in the other 30 mass directions.

The lower bounds on the gluino mass strongly depends on the stop mass and is relatively more severe around $1.0\ \text{TeV} < m_{\tilde{t}_1} < 2.5\ \text{TeV}$. This is because there is no search channel within the set in Table II, which probes

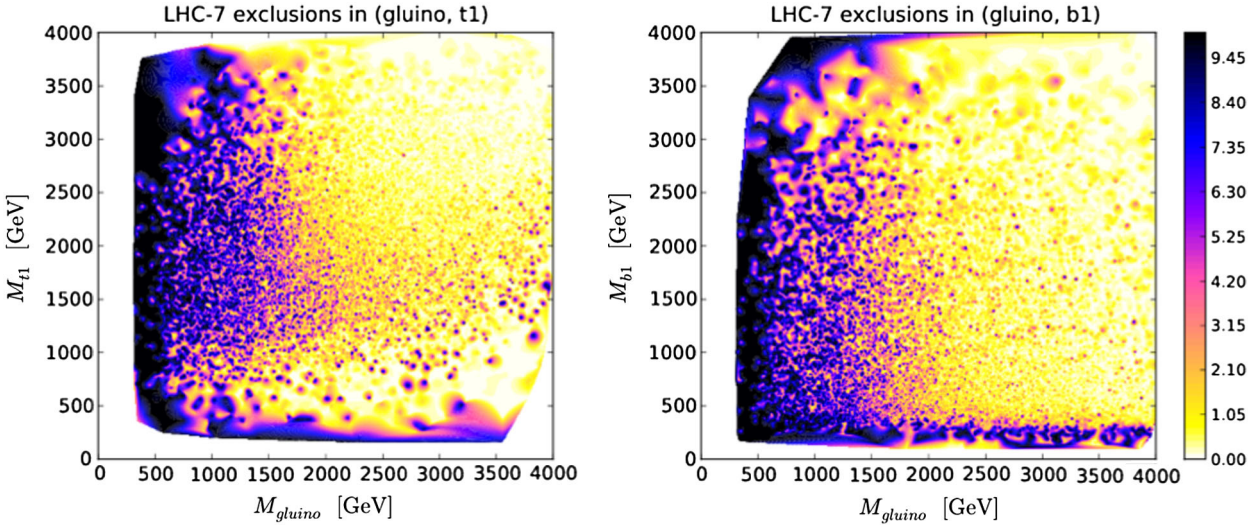

FIG. 2 (color online). The plots show 95% confidence level exclusion contours for gluino-stop and gluino-sbottom mass planes derived from the combined set of ATLAS limits. The color scales are proportional to the expected number of signal events normalized to the combined exclusion limit. The contour max $(\frac{\sigma^{\rm acc}}{\sigma^{\rm cutoff}}) = 1.0$ determines the exclusion boundaries within the sparticle masses plane. Regions with color code greater than unity are excluded at 95% confidence level.

the light (sub-TeV) stop regions unlike the case for the sbottom, which is probed by two b-tagged channels from Refs. [8,14]. Another effect contributing to the irregular nature of Fig. 2(a) compared to Fig. 2(b) is the nature of the posterior probability distributions. The $m_{\tilde{t}_1}$ is widely distributed with values centred around 2 TeV unlike $m_{\tilde{b}_1}$ which are mostly in the sub-TeV range. Figure 2(a) shows that, unlike the gluino mass which is now constrained to be heavy $\sim$3 TeV as revealed by the Bayesian probability distributions in Fig. 1, the third generation squarks can be much lighter (sub-TeV magnitudes.) In fact Fig. 2(a) reveals that sub-TeV gluinos are not ruled out in the relatively less likely (as can be seen in the corresponding posterior distributions in Fig. 1 light stops scenario.

IV. CONCLUSIONS AND OUTLOOK

We have computed the effect of SUSY search results from ATLAS Collaboration with up to 4.7 fb^{-1} of 7 TeV LHC data sets taken during the year 2011. This is done by simulating SUSY events at the LHC with HERWIG++ [58] and the experimental analyses of the data with RIVET [61]. The particle-level per-event RIVET analysis is used for calculating the pMSSM predictions for the cross section within acceptances of the analyses' cuts and events selection criteria. Comparison with the experimental 95% C.L. upper limits (shown in Table II) rules out about 40% of the initial pMSSM sample from a pre-LHC global fit to data. The SUSY limits are most sensitive in constraining the gluino mass whose distribution is now centred around 3 TeV (shifted from 2 TeV). There is also a shift, but less significant compared to the gluino mass case, in preference for heavier first- or second-generation and stop masses as can be seen in the posterior distributions in Fig. 1. The excluded versus allowed regions by the ATLAS's extra-SM cross section upper limits on the gluino-stop and gluino-sbottom mass planes are shown in Fig. 2.

Combining the SUSY and Higgs boson discovery data as described in Ref. [63] further constrains the pre-LHC posterior samples as summarized in Table III with only a single point (out of the initially about 40000 pre-LHC posterior sample points) surviving all of the following requirements:

$$\text{SUSY } \sigma^{\rm acc} \text{ upper limits},$$
$$m_h = 125\text{–}126.5 \text{ GeV}, \quad \text{and}$$
$$R_{ZZ;\gamma\gamma} \equiv \frac{\mu_{ZZ}}{\mu_{\gamma\gamma}} = 0.56 \pm 0.25.$$

Here $\mu_X = \frac{\sigma(gg\to h)\text{Br}(h\to X)}{\sigma(gg\to h)_{\rm SM}\text{Br}(h\to X)_{\rm SM}}$ where $X = \gamma\gamma$ or ZZ. The spectrum is characterized with a quasidegenerate sbottom and LSP and heavy gluino and first- or second-generation squarks. It is the difficult-to-see type at the LHC, discussed in Refs. [50,66]. It is worth mentioning that the data from the Higgs sector (4.67% model points survived) is far more constraining compared to the SUSY limits (57.47% model points survived). There is, however, some complementarity between the two sets of constraints since applying the SUSY limits on the Higgs data surviving model points brings down the surviving number to 2.19%.

Our results go beyond the 1 fb^{-1} analysis done in Ref. [21] from various perspectives. First, our pre-LHC prior construction takes into account the constraint on the neutralino LSP relic density. We use the more stringent

TABLE IV. The status of SUSY snow mass points and slopes benchmarks [67] predicted with our LO calculations (top values) compared to the NLO done in [26] (bottom values). The conservative nature of the LO results manifests for the SPS4 case, which is rather ruled out by the NLO calculations. Note the agreements for the SPS9 cross sections which are all computed at LO.

	σ/pb				Status
Benchmark point	A	B	C	D	ATLAS 35 pb^{-1}
ATLAS limits	1.3	0.35	1.1	0.11	
sps1a	1.347	0.640	1.172	0.299	A, B, C, D
	2.031	0.933	1.731	0.418	A, B, C, D
sps1b	0.077	0.057	0.062	0.041	Allowed
	0.120	0.089	0.098	0.067	Allowed
sps2	0.499	0.280	0.425	0.169	D
	0.674	0.388	0.584	0.243	B, D
sps3	0.079	0.059	0.061	0.043	Allowed
	0.123	0.093	0.097	0.067	Allowed
sps4	0.218	0.132	0.195	0.084	Allowed
	0.334	0.199	0.309	0.144	D
sps5	0.468	0.259	0.417	0.125	D
	0.606	0.328	0.541	0.190	D
sps6	0.523	0.289	0.411	0.149	D
	0.721	0.416	0.584	0.226	B, D
sps7	0.007	0.005	0.008	0.005	Allowed
	0.022	0.016	0.023	0.015	Allowed
sps8	0.011	0.005	0.015	0.003	Allowed
	0.021	0.011	0.022	0.009	Allowed
sps9	0.015	0.003	0.004	0.001	Allowed
	0.019	0.004	0.006	0.002	Allowed

ATLAS SUSY limits from up to 4.7 fb^{-1} of data, which include channels that better constrain gluino production with subsequent decay chains with several jets in the final states.

The results and conclusions obtained from our analyses are conservative. This is because the SUSY signal simulations were done at leading order (LO) in perturbative QCD as opposed to the next-to-leading order (NLO) results reported by ATLAS. Since the NLO cross sections are generally greater compared to the LO values, the exclusions here are more conservative. We will be allowing points that otherwise will be ruled out as is the case for the SPS4 benchmark point in Table IV, where the LO and NLO cross sections within acceptance for snow mass points and slopes benchmark points can be compared. There is an approximate agreement, within the expected $\sim$50% accuracies, with the corresponding values obtained by previous computations (with NLO corrections) [26].

For the analysis here, only the posterior samples from a pre-LHC global fit to data with a logarithmic prior distribution over the 20 pMSSM parameters were considered. No analysis is done with the flat prior sample because it knows that the pre-LHC fits were prior dependent. However, it will be interesting [68] to estimate the strength of the LHC data by checking whether it allows for prior independent results, which is necessarily needed for making conclusions regarding the predictive power of the pMSSM. This seems possible given the apparent interplay between Higgs boson decay rate in the di-photon decay channels, which would require light sparticles[4] and the absence of a SUSY signal to date at the LHC.

ACKNOWLEDGMENTS

Thanks to D. Choudhury, F. Quevedo and D. Grellscheid for helpful comments and discussions and to the IPPP for hospitality during the early stage of this project.

[4]Assuming that R-parity conserving MSSM is responsible for the physics behind the observed deviation from the SM model expectation in the di-photon channel.

[1] G. Aad *et al.* (ATLAS Collaboration), Phys. Lett. B **716**, 1 (2012).
[2] S. Chatrchyan *et al.* (CMS Collaboration), Phys. Lett. B **716**, 30 (2012).
[3] P. Nath, arXiv:hep-ph/0307123.
[4] D. Alves *et al.* (LHC New Physics Working Group Collaboration), J. Phys. G **39**, 105005 (2012).
[5] G. Aad *et al.* (Atlas Collaboration), Phys. Lett. B **701**, 186 (2011).
[6] G. Aad *et al.* (ATLAS Collaboration), Eur. Phys. J. C **71**, 1682 (2011).
[7] ATLAS Collaboration, Report No. ATLAS-CONF-2011-090, 2011.
[8] ATLAS Collaboration, Report No. ATLAS-CONF-2011-098, 2011.
[9] G. Aad *et al.* (ATLAS Collaboration), Phys. Lett. B **710**, 67 (2012).
[10] G. Aad *et al.* (Atlas Collaboration), J. High Energy Phys. 11 (2011) 099.
[11] ATLAS Collaboration, Report No. ATLAS-2012-CONF-2012-033, 2012.
[12] ATLAS Collaboration, Report No. ATLAS-2012-CONF-2012-037, 2012.
[13] ATLAS Collaboration, Report No. ATLAS-2012-CONF-2012-041, 2012.
[14] G. Aad *et al.* (ATLAS Collaboration), Phys. Rev. D **85**, 112006 (2012).
[15] G. Aad *et al.* (ATLAS Collaboration), Phys. Rev. Lett. **108**, 261804 (2012).
[16] C. Balazs, A. Buckley, D. Carter, B. Farmer, and M. White, arXiv:1205.1568.
[17] B. C. Allanach, T. J. Khoo, and K. Sakurai, J. High Energy Phys. 11 (2011) 132.
[18] O. Buchmueller *et al.*, Eur. Phys. J. C **72**, 1878 (2012).
[19] O. Buchmueller, R. Cavanaugh, M. Citron, A. De Roeck, M. J. Dolan, J. R. Ellis, H. Flacher, S. Heinemeyer *et al.*, Eur. Phys. J. C **72**, 2243 (2012).
[20] P. Bechtle, T. Bringmann, K. Desch, H. Dreiner, M. Hamer, C. Hensel, M. Kramer, N. Nguyen *et al.*, J. High Energy Phys. 06 (2012) 098.
[21] S. Sekmen, S. Kraml, J. Lykken, F. Moortgat, S. Padhi, L. Pape, M. Pierini, H. B. Prosper, and M. Spiropulu, J. High Energy Phys. 02 (2012) 075.
[22] M. W. Cahill-Rowley, J. L. Hewett, S. Hoeche, A. Ismail, and T. G. Rizzo, Eur. Phys. J. C **72**, 2156 (2012).
[23] M. Carena, J. Lykken, S. Sekmen, N. R. Shah, and C. E. M. Wagner, Phys. Rev. D **86**, 075025 (2012).
[24] A. Arbey, M. Battaglia, and F. Mahmoudi, Eur. Phys. J. C **72**, 1847 (2012).
[25] M. E. Cabrera, J. A. Casas, V. A. Mitsou, R. R. de Austri, and J. Terron, J. High Energy Phys. 04 (2012) 133.
[26] M. J. Dolan, D. Grellscheid, J. Jaeckel, V. V. Khoze, and P. Richardson, J. High Energy Phys. 06 (2011) 095.
[27] D. Grellscheid, J. Jaeckel, V. V. Khoze, P. Richardson, and C. Wymant, J. High Energy Phys. 03 (2012) 078.
[28] A. Fowlie, A. Kalinowski, M. Kazana, L. Roszkowski, and Y. L. S. Tsai, Phys. Rev. D **85**, 075012 (2012).
[29] A. Fowlie, M. Kazana, K. Kowalska, S. Munir, L. Roszkowski, E. M. Sessolo, S. Trojanowski, and Y.-L. S. Tsai, Phys. Rev. D **86**, 075010 (2012).
[30] C. Strege, G. Bertone, D. G. Cerdeno, M. Fornasa, R. R. de Austri, and R. Trotta, J. Cosmol. Astropart. Phys. 03 (2012) 030.
[31] R. Essig, E. Izaguirre, J. Kaplan, and J. G. Wacker, J. High Energy Phys. 01 (2012) 074.
[32] Y. Kats, P. Meade, M. Reece, and D. Shih, J. High Energy Phys. 02 (2012) 115.
[33] C. Brust, A. Katz, S. Lawrence, and R. Sundrum, J. High Energy Phys. 03 (2012) 103.
[34] M. Papucci, J. T. Ruderman, and A. Weiler, J. High Energy Phys. 09 (2012) 035.
[35] R. Aaij *et al.* (LHCb Collaboration), Phys. Rev. Lett. **108**, 231801 (2012).
[36] M. Verzocchi, in *Proceedings of 34th International Conference in High Energy Physics (ICHEP08), Philadelphia, 2008* (SLAC National Accelerator Laboratory, Menlo Park, CA, 2008).
[37] ALEPH Collaboration, Phys. Rep. **427**, 257 (2006).
[38] G. W. Bennett *et al.* (Muon G-2 Collaboration), Phys. Rev. D **73**, 072003 (2006).
[39] M. Davier, Nucl. Phys. B, Proc. Suppl. **169**, 288 (2007).
[40] E. Barberio *et al.* (Heavy Flavor Averaging Group (HFAG) Collaboration), arXiv:0704.3575.
[41] A. Abulencia *et al.* (CDF Collaboration), Phys. Rev. Lett. **97**, 242003 (2006).
[42] B. Aubert *et al.* (*BABAR* Collaboration), Phys. Rev. Lett. **95**, 041804 (2005).
[43] P. Chang, in *Proceedings of 34th International Conference in High Energy Physics (ICHEP08), Philadelphia, 2008* (SLAC National Accelerator Laboratory, Menlo Park, CA, 2008).
[44] A. Gray, M. Wingate, C. Davies, E. Gulez, G. Lepage, Q. Mason, M. Nobes, and J. Shigemitsu (HPQCD Collaboration), Phys. Rev. Lett. **95**, 212001 (2005).
[45] C. Amsler *et al.* (Particle Data Group Collaboration), Phys. Lett. B **667**, 1 (2008).
[46] E. Komatsu *et al.* (WMAP Collaboration), Astrophys. J. Suppl. Ser. **180**, 330 (2009).
[47] S. S. AbdusSalam, B. C. Allanach, F. Quevedo, F. Feroz, and M. Hobson, Phys. Rev. D **81**, 095012 (2010).
[48] S. S. AbdusSalam, AIP Conf. Proc. **1078**, 297 (2008).
[49] S. S. AbdusSalam and F. Quevedo, Phys. Lett. B **700**, 343 (2011).
[50] S. S. AbdusSalam, Phys. Lett. B **705**, 331 (2011).
[51] S. S. AbdusSalam, B. C. Allanach, H. K. Dreiner, J. Ellis *et al.*, Eur. Phys. J. C **71**, 1835 (2011).
[52] K. L. Chan, U. Chattopadhyay, and P. Nath, Phys. Rev. D **58**, 096004 (1998).
[53] G. Aad *et al.* (ATLAS Collaboration), Eur. Phys. J. C **72**, 2174 (2012).
[54] G. Aad *et al.* (ATLAS Collaboration), Phys. Lett. B **718**, 841 (2013).
[55] ATLAS Collaboration, Report No. ATLAS-2012-CONF-2012-103, 2012.
[56] ATLAS Collaboration, Report No. ATLAS-2012-CONF-2012-104, 2012.
[57] ATLAS Collaboration, Report No. ATLAS-2012-CONF-2012-109, 2012.

[58] M. Bahr, S. Gieseke, M. A. Gigg, D. Grellscheid, K. Hamilton, O. Latunde-Dada, S. Platzer, and P. Richardson *et al.*, Eur. Phys. J. C **58**, 639 (2008).
[59] S. Gieseke *et al.*, arXiv:1102.1672.
[60] B. C. Allanach, Comput. Phys. Commun. **143**, 305 (2002).
[61] A. Buckley, J. Butterworth, L. Lonnblad, H. Hoeth, J. Monk, H. Schulz, J. E. von Seggern, F. Siegert *et al.*, arXiv:1003.0694.
[62] M. Cacciari, G. P. Salam, and G. Soyez, Eur. Phys. J. C **72**, 1896 (2012).
[63] S. S. AbdusSalam and D. Choudhury, arXiv:1210.3331.
[64] P. Bechtle, O. Brein, S. Heinemeyer, G. Weiglein, and K. E. Williams, Comput. Phys. Commun. **181**, 138 (2010).
[65] G. Degrassi, S. Heinemeyer, W. Hollik, P. Slavich, and G. Weiglein, Eur. Phys. J. C **28**, 133 (2003).
[66] T. J. LeCompte and S. P. Martin, Phys. Rev. D **84**, 015004 (2011).
[67] B. C. Allanach, M. Battaglia, G. A. Blair, M. S. Carena, A. De Roeck, A. Dedes, A. Djouadi, D. Gerdes *et al.*, Eur. Phys. J. C **25**, 113 (2002).
[68] S. S. AbdusSalam *et al.* (unpublished).